Tight binding simulations of tetragonal $MAPbI_3$ domains within orthorhombic phase

A. Di Vito[†,*], A. Pecchia[‡], M. Auf der Maur[†], A. Di Carlo[†,§]
[†]Department of Electronics Engineering, University of Rome Tor Vergata, Via del Politecnico 1, 00133 Rome, Italy
[‡]CNR-ISMN, Via Salaria km 29.300, 00017 Monterotondo, Rome, Italy
[§]CNR-ISM, Via del Fosso del Cavaliere 100, 00133 Rome, Italy
[*]Email: alessia.di.vito@uniroma2.it

***Abstract*—Very recent photoluminescence studies, investigating the tetragonal-to-orthorhombic phase transition of $MAPbI_3$, demonstrated the presence of residual tetragonal phase far below the transition temperature, yielding spectral signatures from quantum confined tetragonal domains. We present a theoretical model of the coexistence of tetragonal and orthorhombic $MAPbI_3$, based on tight binding simulations. The tight binding parameters are derived by particle swarm optimization and the band-offset between the two crystals is obtained by first-principles calculations. The impact of the tetragonal domain dimension on the optical properties of $MAPbI_3$ is discussed.**

I. Introduction

In the last years, the most important breakthrough in the field of photovoltaics is represented by hybrid metal halide perovskites. These materials exhibit the presence of two phase transitions occurring in the temperature range of technologically relevant applications. Concerning the prototypical methylammonium lead iodide perovskite ($MAPbI_3$), experimental investigations [1] highlighted the presence of an orthorhombic-to-tetragonal phase transition at 162 K and a tetragonal-to-cubic phase transition at 327 K.

Interestingly, recent temperature-dependent photoluminescence (PL) measurements [2] demonstrated that a fraction of residual tetragonal phase is still present down to 120 K even in the case of a single crystal. Specifically, they observed PL signatures from quantum confined tetragonal domains, suggesting their size to be about 7-15 nm down to 120 K.

Here, we present the results obtained by tight binding (TB) simulation of nanometric tetragonal $MAPbI_3$ domains within the orthorhombic phase. We analyze the impact of the tetragonal domain dimension on the optical properties of $MAPbI_3$ perovskite. The computational details are reported in Section II and the results are discussed in Section III.

II. Computational Approach

The electronic and optical properties of the system have been described at the atomic scale level using the TB approach as implemented in the TiberCAD software [3]. The choice of TB basis can be the minimal sp^3 set, as demonstrated by Boyer-Richard et al. [4]. Moreover, the TB model does not include the MA cation, consistently with density functional theory (DFT) studies of the electronic states around the band gap that do not reveal significant weight stemming from MA [5]. We evaluated the first twelve electron and the first twelve hole states from which we calculated the momentum matrix elements and optical spectra. The G, X, Z, M, R and A k points of the Brillouin zone are considered and we used the trapezoidal method for reciprocal space integration. The orthorhombic $MAPbI_3$ box is fixed to 25 nm and the tetragonal domain is placed at the center of the box. The considered domain dimensions are 5, 9 and 14 nm, consistently with the estimate of Schötz *et al.* [2].

TABLE I
Energy gap values (eV) obtained with TB after PSO for orthorhombic and tetragonal $MAPbI_3$. The results are compared with the experimental and theoretical values obtained by Quarti *et al.* [6].

	orthorhombic	tetragonal
TB (after PSO)	1.82	1.78
DFT-GW [6]	1.81	1.67
Experiment [6]	1.65	1.61

We employed the particle swarm optimization (PSO) algorithm [7] for the parameterization of the TB Hamiltonian matrix elements using the DFT band dispersion as a target [8]. The energy gap values obtained by TB simulations after PSO are listed in Table I and compared with the experimental and state-of-art GW calculations of Quarti *et al.* [6].

The valence band (VB) offset between tetragonal and orthorhombic $MAPbI_3$ is derived by first-principles calculations, based on the DFT reference study of Weston *et al.* [9]. We obtain a VB offset of 0.01 eV, thus, the conduction band (CB) discontinuity is equal to 0.03 eV, i.e. the band gap difference between the two materials minus the VB offset. The band alignments are sketched in Figure 1.

III. Results and Discussion

In Figure 2, the normalized emission spectra calculated at 150 K for the three considered dimensions of the tetragonal domain are reported. We can observe an important red-shift of the peak emission energy for the 14 nm domain size. This means that the energy gap is significantly reduced for the 14 nm tetragonal domain system. In this case, depicted by the red solid line in Figure 2, both the peaks from the tetragonal and the orthorhombic crystals are visible. On the other hand, the difference in the calculated spectra between the 5 nm and the

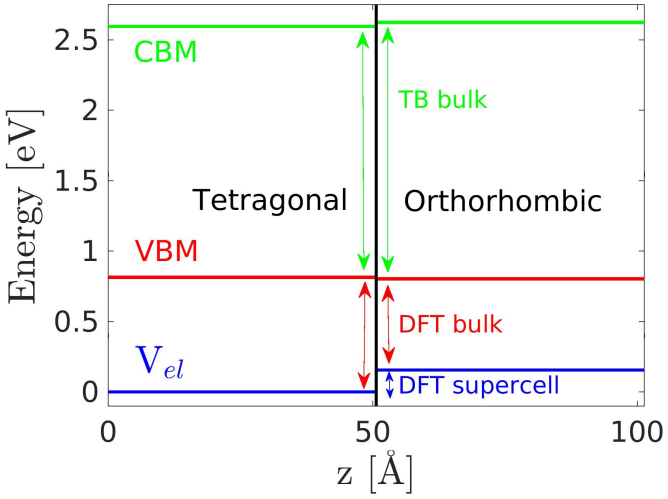

Fig. 1. Band alignments between tetragonal and orthorhombic $MAPbI_3$ derived by the combination of bulk and superlattice DFT calculations [9]. The conduction band discontinuity is obtained considering the TB band gap values.

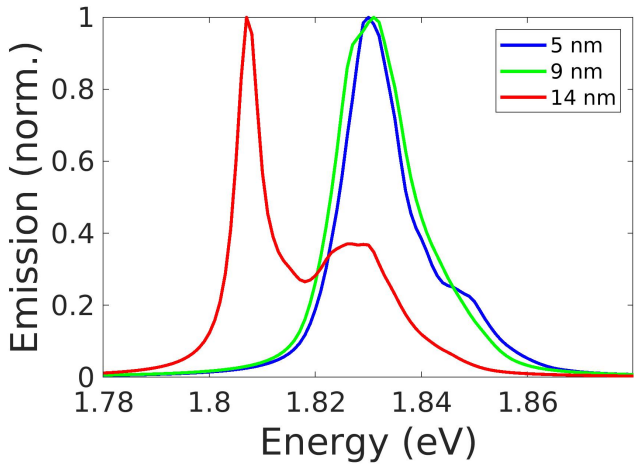

Fig. 2. Emission spectra calculated at 150 K for the three considered tetragonal domain dimensions.

9 nm domain size is not relevant, since the tetragonal domain dimension is not sufficient to induce spatial localization of the electron ground state in these cases.

The observed features are due to the spatial localization of the ground state electron wave function within the tetragonal domain, for the largest considered domain size. This is depicted in panel b) of Figure 3, where the isosurface containing the 50% of the total ground state density of the electron is shown for the 14 nm tetragonal domain system. In panel a) of the Figure, the same quantity is represented for the 5 nm domain system. Even if the isosurface in panel a) contains only the 10% of the total ground state density, we can see that the electron wave function is not localized within the tetragonal crystal. As the conduction band discontinuity is much more pronounced than the valence band one, the localization effect is not observed for the ground state hole wave function and

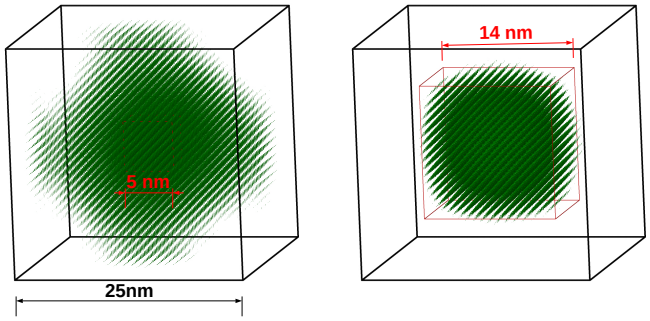

Fig. 3. Ground state electron wave function for a) the 5 nm and b) the 14 nm tetragonal domain system. The isosurfaces containing a) 10% and b) 50% of the total ground state density are shown.

the valence band maximum value is almost unaffected by the dimension of the tetragonal domain. Thus, the energy gap reduction originates from the localization of the electron ground state within the low-band-gap tetragonal crystal.

References

[1] A. Poglitsch and D. Weber, "Dynamic disorder in methylammoniumtrihalogenoplumbates (ii) observed by millimeter-wave spectroscopy," *The Journal of chemical physics*, vol. 87, no. 11, pp. 6373–6378, 1987.

[2] K. Schötz, A. M. Askar, A. Köhler, K. Shankar, and F. Panzer, "Investigating the tetragonal-to-orthorhombic phase transition of methylammonium lead iodide single crystals by detailed photoluminescence analysis," *Advanced Optical Materials*, p. 2000455, 2020.

[3] "TiberCAD simulation package," http://www.tibercad.org.

[4] S. Boyer-Richard, C. Katan, B. Traore, R. Scholz, J.-M. Jancu, and J. Even, "Symmetry-based tight binding modeling of halide perovskite semiconductors," *The journal of physical chemistry letters*, vol. 7, no. 19, pp. 3833–3840, 2016.

[5] J. Even, L. Pedesseau, J.-M. Jancu, and C. Katan, "Importance of spin–orbit coupling in hybrid organic/inorganic perovskites for photovoltaic applications," *The Journal of Physical Chemistry Letters*, vol. 4, no. 17, pp. 2999–3005, 2013.

[6] C. Quarti, E. Mosconi, J. M. Ball, V. D'Innocenzo, C. Tao, S. Pathak, H. J. Snaith, A. Petrozza, and F. De Angelis, "Structural and optical properties of methylammonium lead iodide across the tetragonal to cubic phase transition: implications for perovskite solar cells," *Energy & Environmental Science*, vol. 9, no. 1, pp. 155–163, 2016.

[7] J. Kennedy and R. Eberhart, "Particle swarm optimization," in *Proceedings of ICNN'95 - International Conference on Neural Networks*, vol. 4, 1995, pp. 1942–1948 vol.4.

[8] A. Di Vito, A. Pecchia, M. A. der Maur, and A. Di Carlo, "Tight binding parameterization through particle swarm optimization algorithm," in *2020 International Conference on Numerical Simulation of Optoelectronic Devices (NUSOD)*. IEEE, 2020, pp. 113–114.

[9] L. Weston, H. Tailor, K. Krishnaswamy, L. Bjaalie, and C. Van de Walle, "Accurate and efficient band-offset calculations from density functional theory," *Computational Materials Science*, vol. 151, pp. 174–180, 2018.